Proceedings Paper:
French, R., Marin-Reyes, H., Kapellmann-Zafra, G. et al. (1 more author) (2019) Robotic additive manufacturing system featuring wire deposition by electric arc for high-value manufacturing. In: Proceedings of 2019 IEEE 15th International Conference on Automation Science and Engineering (CASE). 2019 IEEE 15th International Conference on Automation Science and Engineering (CASE) , 22-26 Aug 2019, Vancouver, BC, Canada. IEEE . ISBN 9781728103570

https://doi.org/10.1109/COASE.2019.8842997

Robotic additive manufacturing system featuring wire deposition by electric arc for high-value manufacturing

Richard French[1], Hector Marin-Reyes[2], Gabriel Kapellmann-Zafra[3], Samantha Abrego-Hernandez[4]

***Abstract*— Increasing demand from the high-value manufacturing industries of quality, productivity, efficiency and security aligns with the ambition and driving need for novel automated robotic systems. This paper describes the motivation, design and implementation phases of the SERFOW project (Smart Enabling Robotics driving Free Form Welding). SERFOW is an automated additive manufacturing arc and wire tungsten inert gas (TIG) welding prototype to support industrial manufacturing requirements of the nuclear, aerospace and automotive industry sectors. Key innovations are found in the integration of a 3D vision system with a robotic manipulator to perform automatic free-form fusion welding for the multiple layer additive material build-up required to expand Additive Manufacturing (AM) with minimum human intervention. Welding trials were performed on samples made of Super Duplex stainless steel alloy. Metallographic observations were performed to analyze the porosity distribution and penetration on the material after welding. Also, temperature, feritescope and tensile measurements were performed. The results showed that the welding and AM process performed with the SERFOW cell are within an acceptable quality tolerance range according to the ISO 5817 and the ASME A789 welding standards.**

I. INTRODUCTION

Additive Manufacturing is defined as the process to join materials by a multi-layer build-up process where the information to build objects could be gathered from a three dimensional (3D) model data [1], [2]. Different types of AM can be found within the high-value manufacturing industries e.g. powder bed fusion, extrusion-based system, material jetting and directed energy deposition processes [3]. AM has the potential to redefine manufacturing processes since it could help to reduce material waste, production steps and the number of distinct parts needed [4]. Therefore the importance of smart manufacturing process development to meet the future industry demands. European governments are steadily investing in the research and development of AM processes for adoption in different industries; aiming to achieve zero waste and more efficient production of metal products by reducing the cost of the manufactured parts in comparison with the traditional methods. This paper aims to showcase a dynamic free form robotic welding system that is capable of providing low-cost AM. The machine prototype has to be autonomous and flexible to perform wire deposition by electric arc AM, also known as Wire and Arc Additive Manufacturing (WAAM) [4], using an advanced stereo camera with auto-focus capabilities, a robotic manipulator and welding power supply. Flexibility is provided by a six-axis robotic arm, enabling the production of structures using metallic additive filler deposition or material joining operations when required. A vision system is implemented to detect and assess the different shapes of the welded components and ensures the correct and accurate position of the robot. The whole system is designed to be integrated with different types of welding technologies, such as laser and plasma welding, and with further development, capable of working on parts of all profiles, shapes and sizes autonomously, which is currently beyond commercially available technologies capability.

The development of new automated AM technologies, as depicted here, allows for rapid, dynamic adaption of production tasks, reducing the high financial penalties of more complex traditional systems. The robotic process provides greater system control during the welding process. The integrated demonstrator will allow the repair and manufacture of high-value industry components found in the nuclear, aerospace and automotive sectors which is of critical importance due to the increasing dependency on bespoke parts consisting of unique shapes, profiles and sizes.

Existing methods used in manufacturing require manual or pre-programmed tasks which could be inflexible and time-consuming [5]. Procedures designed for mass production of the same unit component are challenged when an updated or a new component is required. Updates are often expensive due to the need of new jigs and fixtures combined with increased set-up time, and additional risk from human error [6], [7], [8]. The prototype system presented in this paper emulates the high skills of experienced fusion welding engineers who can manually build-up layers of additive filler wire onto complex shape objects [9]. A representative cooling manifold assembly fabricated from Super Duplex stainless steel comprises of a mounting block, connecting tube and an inlet port. This component assembly, known as heat exchanger manifold, is used to demonstrate the prototype systems material joining and build-up AM capability, as shown in Fig. 1. The SERFOW prototype was constructed in the Enabling Sciences for Intelligent Manufacturing (ESIM) Laboratory of the Physics and Astronomy department at the University of Sheffield. An extruded aluminium profile chassis structure houses the robotic, AM and vision systems.

This work was supported by Innovate UK, project reference 103462.

[1]Richard French is with the Department of Physics and Astronomy, The University of Sheffield, Sheffield, United Kingdom r.s.french@sheffield.ac.uk

[2]Hector Marin-Reyes is with the Department of Physics and Astronomy, The University of Sheffield, Sheffield, United Kingdom H.Marin-Reyes@sheffield.ac.uk

[3] Gabriel Kapellmann-Zafra is with the Department of Physics and Astronomy, The University of Sheffield, Sheffield, United Kingdom g.kapellmann@sheffield.ac.uk

[4] Samantha Abrego-Hernandez is with the Department of Physics and Astronomy, The University of Sheffield, Sheffield, United Kingdom s.abrego@sheffield.ac.uk

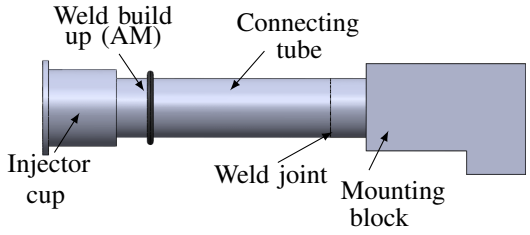

Fig. 1. 3D CAD rendering of components of a heat exchanger manifold.

The key design development was to provide a flexible and adaptable structure for future projects. Modules of the system comprised of an Universal Robots UR-10 six-degrees-of-freedom robot arm combined with a Shadow Robot Smart Grasping System (SGS) [10], [11].

The robotic elements, UR10 robot arm and SGS, position the pieces to weld into a re-orientation jig first to ensure the correct orientation. Then these pieces are taken from the re-orientation jig to the rotary turn-table controlled by I3D Robotics (I3DR) stereo vision systems: Phobos [12] and PosCam cameras. AM and arc welding are conducted by an industry standard TIG welding system described in section V. Automatic movements of the welding system (wire feeder and torch) are controlled by two linear motor drives in the "X" and "Z" axis. Fig. 2, shows an image of the described components when fully assembled.

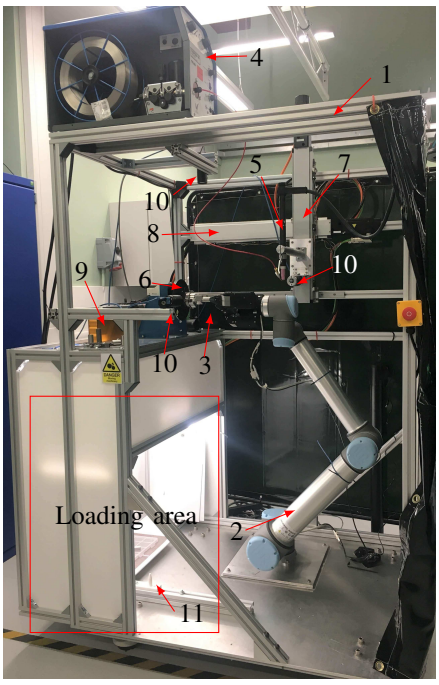

Fig. 2. SERFOW cell: 1) aluminum structure, 2) robotic arm, 3) smart grasper, 4) wire feeder, 5) torch, 6) turn-table, 7) Z axis linear motor drive, 8) X axis linear motor drive, 9) Phobos camera, 10) PosCam cameras, 11) re-orientation jig.

II. Vision System for Intelligent Welding

The 3D stereo vision system proposed and implemented in this paper interacts with the robotic grasping and welding systems by two subsystems called Phobos and PosCam cameras. The shape, profile and depth information of the objects are acquired by the 3D vision system to undergo manufacturing. Additionally, the vision system confirms correct grasping, real-time monitoring and feedback to control the welding conditions such as the AM filler wire delivery speed and arc voltage control. Information is delivered to the robot for both trajectories and path planning execution.

A. Phobos vision system

Stereo vision produces a 3D model of an object or a target area by matching features between two or more images of the scene. This is known as the correspondence problem and is solved using a stereo matching algorithm such as in [13], followed by [14], [15]. There is an increasing number of published matching algorithms [16], most of which employ some form of correlation between points in the image pairs. Stereo images are usually rectified, such that corresponding features lie on the same pixel line in each image [17]. Stereo vision utilises 3D points in space which project to distinct 2D pixel locations in images of the scene when acquired from two different locations. The differences in pixel coordinates in the images allow reconstruction of the 3D coordinates from the images.

Following a calibration process, the stereo algorithm processes the image-pairs and produces a 3D point cloud. This cloud is effectively a set of data points where each pixel provides disparity or distance information, of the scene. Fig. 3 shows an example of a meshed point cloud where a cylinder can be viewed in a scene on a flat surface with a random background used to calibrate the vision system to provide pixels disparity or distance information. Phobos is

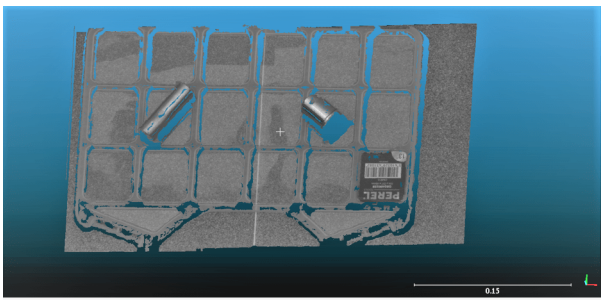

Fig. 3. Example of a point cloud showing a cylindrical object acquired by the Phobos camera.

a high-resolution stereo camera developed by I3DR [12]. It can provide a spatial resolution of 0.11 mm, with a depth resolution of 0.45 mm at 1 m range, over a field of view of 1.06 m x 0.88 m. It is used to recognise and obtain the objects dimensional characteristics (profile, shape and depth) in a target scene. Mounted directly above the components loading area, as shown in Fig. 2, Phobos obtains the positional coordinates of the components to be either joined or to

undergo the AM process. I3DR developed the Phobos software which has been integrated and tested in ROS-Industrial [18]. The positional coordinates obtained were used as an input to control the UR-10 robot and the SGS. This robotic manipulator locates each component, then grasps and loads it into an automated rotary turn-table. The highly reflective nature of metallic components caused illumination problems during initial research and development [19], [20], [21] due to the fact that illuminating directly onto the parts results in reflections where the parts are not illuminated uniformly. The use of a diffused light illumination method was implemented, effectively providing reflected lighting from various angles on white surfaces. By illuminating the white surfaces, some form of diffusion is obtained. Using this new backlighting method allowed for successful part detection to be conducted.

It does remain critical for the system to be appropriately calibrated to minimise reflections on the component, and it is an area for further development.

B. PosCam multicamera system

The PosCam system is composed of three cameras, A, B and C, monochrome industrial cameras, positioned in the welding area as Fig. 4 shows. Camera A was attached to the welding torch holder which moves in X and Z axis. The centre of this camera was aligned with the welding torch electrode tip. This allowed the precise positioning of the torch tip to the work-piece, which is critical for the successful operation of wire deposition by electric arc additive manufacturing. A laser with a power of 0.5 W and a wavelength of 405 nm was passed through a beam expander and a filter band-pass at 405 nm. This wavelength was chosen from the arc spectrum at the lowest wavelength emitted by the welding arc. This will allow to see and monitor the weld pool on the welded piece and the arc welding process with camera A [22].

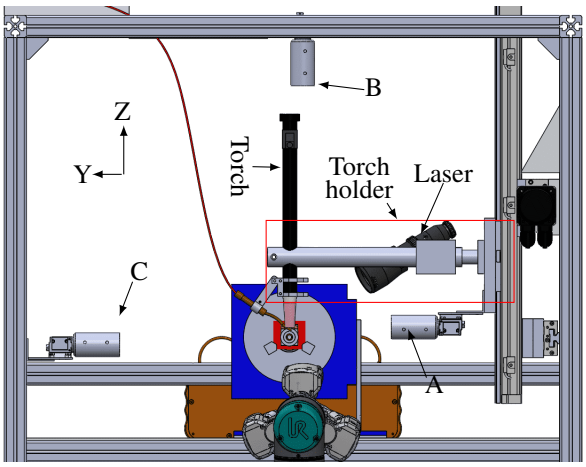

Fig. 4. PosCam system 3D CAD.

Absolute camera precision was determined by the lens choice and working distance. The key parameters were the resolution, field-of-view and depth-of-field because the TIG torch and camera A were fixed relative to each other at 150 mm. Cameras B and C are used to monitor the work-piece position in the turn-table. Camera B was mounted vertically on the aluminium structure, while camera C was fixed horizontally. Once the correct position of the component to weld is confirmed by the cameras A, B and C, the vision system send a signal to the welding system to allow the weld to commence. Fig. 5 shows the images obtained by cameras A and C.

These cameras enabled control over the welding parameters such as voltage, linear welding speed, wire feeder speed and the electrode tip distance. 3D models of the conducted orbital weld and AM layers were produced and monitored by the stereo vision system to give feedback and make any necessary modification in the welding parameters. This is a step forward from a previous collaborative research between the ESIM group and I3D Robotics called the IVIEW project [23].

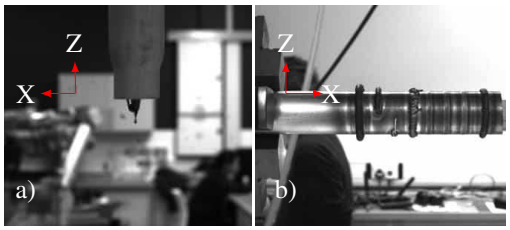

Fig. 5. a) Image acquired by camera A attached to the welding torch, b) Image acquired by fixed camera C attached to the aluminium structure.

III. Smart Grasping System

An UR10 (six-degrees-of-freedom) robot arm and the Shadow's SGS were used to pick-&-place parts in the correct sequence dictated by the recognition patterns and location of Phobos before manufacturing. This was a huge advantage over the current manufacturing processes where usually the grabbing of the pieces had to be done manually or use pre-programmed trajectories by line operators [24].

The main characteristics of the UR10 are its payload mass of 10 Kg and its good repeatable accuracy of 0.1 mm. The UR10, in combination with Shadow's SGS, demonstrate both flexibility and dexterity to manipulate different objects sizes, shapes and weights. This is possible due to the SGS's library of different grasps with torque sensing capabilities on each joint. In this paper, the three-fingered configuration was used because its nine-degrees-of-freedom gives more stability to the assembled parts. However, one of these fingers was modified to have a conical shape, made of Stainless Steel (SS), to help with the alignment of the pieces by holding them when assembled and mounted in the turn-table while the welding process occurs, as depicted in Fig. 6. Furthermore, Shadow's SGS has been proven to tolerate, to a certain degree, exposure to radioactive environments which suggest possible applicability in the nuclear sector [25][26].

IV. System Interfacing and Control

The implementation of this design was been made using ROS for LabVIEW libraries developed by Tufts University

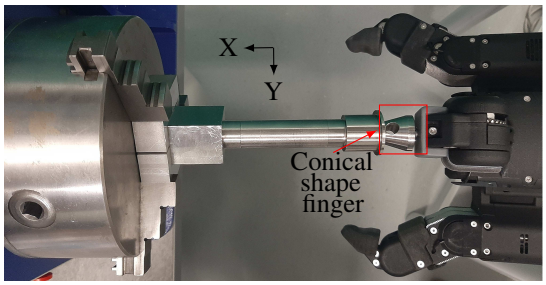

Fig. 6. Shadow Robot SGS aligning heat exchanger with turn-table centre of rotation.

[27], [28], [29]. SERFOW's ROS workflow is shown in Fig. 7. These libraries have the capability of handling node-to-node transport negotiation and communication using the Transmission Control Protocol (TCP). They are also capable of sending and receiving messages from ROS topics/services, coding or decoding message strings, and connecting into a ROS master [18]. The workflow to perform robotic TIG welding and AM is shown in Fig. 8.

V. Automated Additive Manufacturing System

TIG Welding and AM trials on Super Duplex stainless steel samples were conducted with a pulsed main current value of 52 Amps and a background current of 12 Amps. The main time value used was 0.04 sec (25%), and the background time value used was 0.12 sec (75%). The rotatory table was set at 1 revolutions-per-min (RPM), when performing the first weld joint and the first layer of wire, and it is increased to 1.2 RPM when performing the second layer.

The components of the TIG welding system set-up used are as follows:

- Miller TIG power source.
- WeldTec TIG torch.
- Technical ARC automatic wire feeder.
- 0.8 mm outside diameter (OD) wire.

All devices are common in traditional manufacturing industries and the welding parameters were controlled through the remote output control as specified by the power source's manual [30].

Layers of filler wire were applied to a 20 mm Super Duplex stainless steel tube. After two layers of wire the OD is 25mm and its width is 4.8 mm, as shown in Fig. 9.

A. Metallographic observations

The metallographic observations performed in welding showed a uniform porosity distribution according to ISO 6520-1:2007) [31], Fig. 10. The total area of detected pores covers 0.4% of the weld bead, which is below the maximum tolerance of 1% defined by the ISO 5817 [32]. The metallographic observations performed in the two layers AM showed that not enough penetration of heat was made as it can be seen in Fig. 11 b). Future work will look at improving the Welding Procedure Specification (WPS) for satisfactory AM.

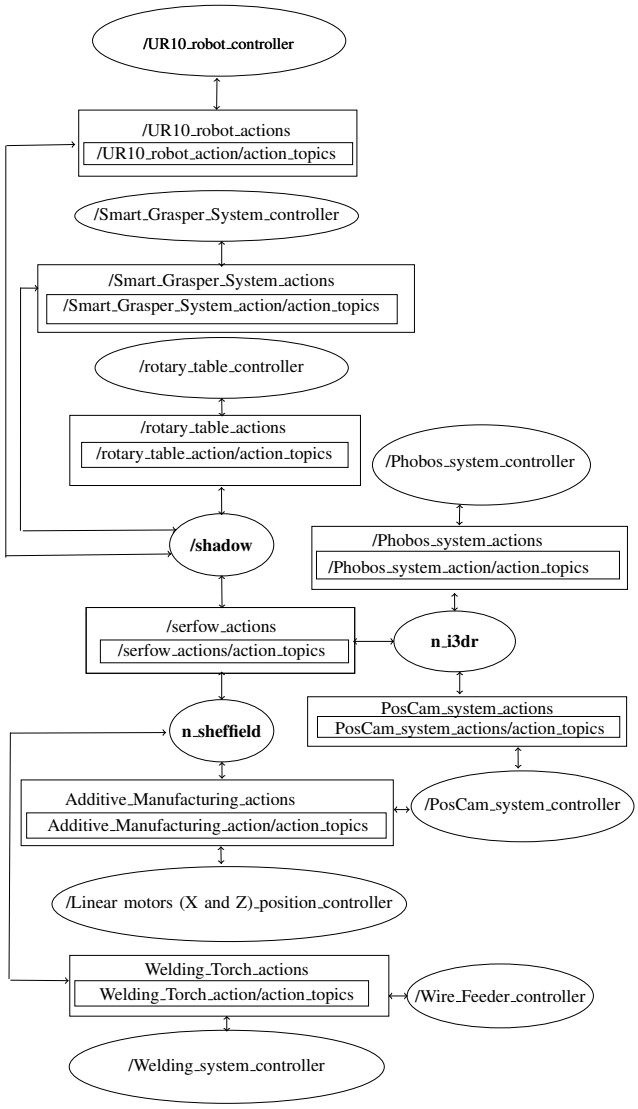

Fig. 7. Diagram showing the ROS nodes and ROS topics workflow used to control the system.

B. Feritscope measurements

The ferrite content affects the mechanical properties, corrosion resistance and weld strength of the materials. In materials such as Super Duplex SS, a deficit of the ferrite content reduce the weld strength and increases the development of stress corrosion cracking [33], [34]. Therefore, measurements of the ferrite content have been performed with MP3C FISCHER Feritscope on the 52-12 samples, as shown in Table I.

TABLE I
Ferrite Content Results

52-12 sample Ferrite content %						Average	Std dev
Side 1	41.1	41.2	39.6	39.7	38.8	40.1	0.9
Side 2	40.3	40.9	40.2	40.7	40.1	40.4	0.3
Weld	50.6	49.4	55.8	49.1	50.9	51.2	2.4

The ferrite content found in the welding trials confirms

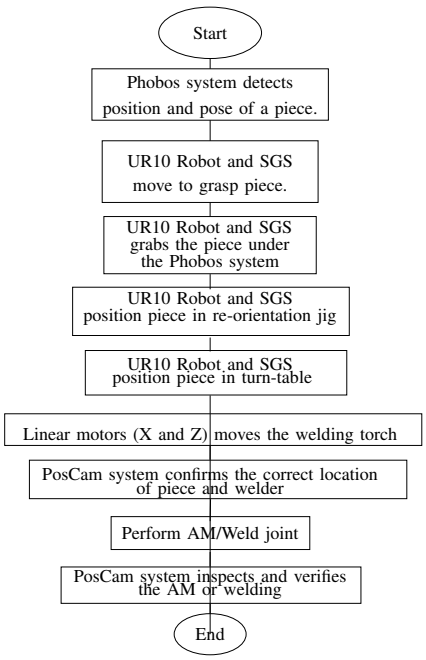

Fig. 8. SERFOW workflow diagram.

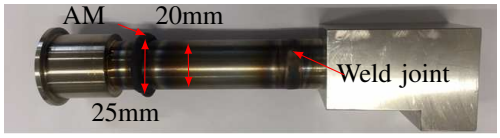

Fig. 9. Heat exchanger trial sample with AM.

that ferrite content is greater in the weld (approximately 51.2%) than in the pipe (approximately 40.4%). Therefore, improvement in the reduction of the ferrite count within the Heat Affected Zone (HAZ) has to be further investigated.

C. Temperature measurements of AM

Temperature measurements of wire deposition of one layer and two layers were taken with a high frame rate thermal camera system capable of taking pictures at 80 frames per second with a radiance range from 750°C to 2000°C to quantify the heat transfer as shown in Fig. 12 [35].

These measurements were made to assess the heat transfer through the SS conic finger-tip of Shadow's SGS, shown in Fig.6, since it holds the piece during the whole AM process. The temperature measurements corroborated that the conical shape SS finger was suitable to withstand the high temperatures during the AM process.

D. Tensile test on fusion joining

Tensile tests on welding sample have been performed on a UTS tensile test machine. Elongation has been measured with stroke displacement only as no extensometer could be fitted. Strength has been estimated on the average of the measured diameter and wall thickness of the pipe extremities. The results obtained are shown in Fig. 13. The tensile test

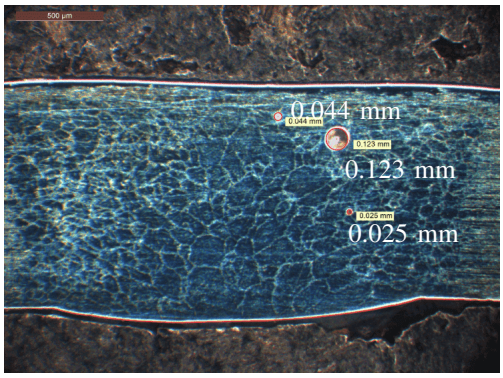

Fig. 10. Metallurgic observations on welding trial of the weld bead with a magnification value of 50x using 52 Amps as back current and 12 Amps as main current.

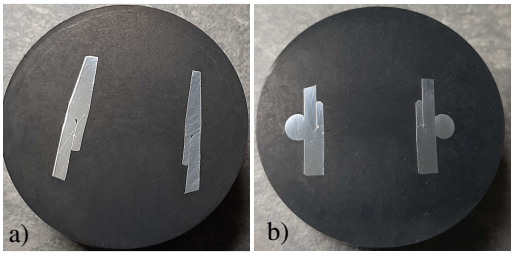

Fig. 11. Metallurgic observations etching preparation on a) TIG welding and b) AM trial

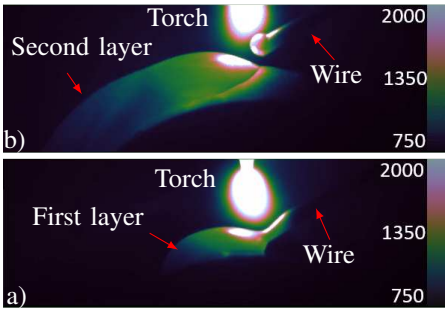

Fig. 12. Temperature measurements [Celsius] of the a) first layer and b) second layer of wire deposition by electric arc.

performed on the three welding samples broke on the weld. The average Ultimate Tensile Strength (UTS) of the samples was 878 $\pm$ 8 MPa. As stated in NFEN 288-3 [36] the UTS should not be less than 800 MPa for UNS S 32750 pipes as stated by in ASTM A789 [37].

VI. CONCLUSIONS AND FUTURE WORK

The fully integrated SERFOW prototype allows for successful automation and implementation of additive manufacturing. The innovative 3D stereo vision system developed for SERFOW accomplished smart grasping and pick-&-place by detecting the position and orientation of work-pieces using I3DR's Phobos and PosCam cameras. The vision system allowed successful processing of the acquired data

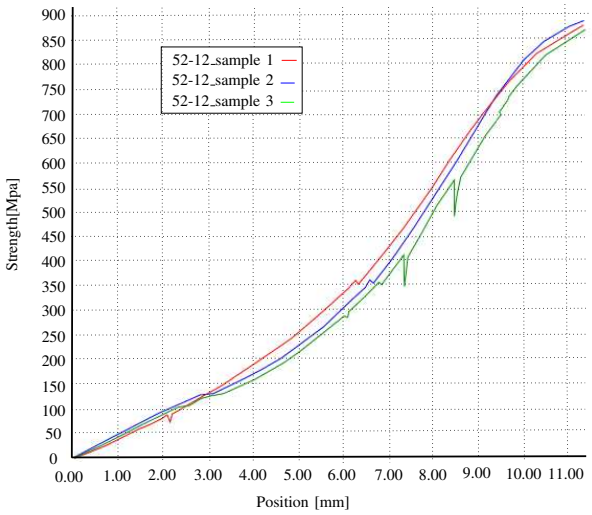

Fig. 13. Tensile test results for 52-12 Super Duplex Stainless Steel welding samples

and transfer of the deduced coordinates to the UR10 robot and Shadow's SGS, interfaced via ROS for LabView. The three-dimensional vision system has also provided effective feedback for the control and monitoring of wire deposition by electric arc. SERFOW effectively delivers both quality checks and accuracy of component production replicating the essential human skills found in fusion welding engineers. The metallurgical analysis performed demonstrates, that while samples which have fusion joining are within an acceptable range according to ISO 5817 ASME A789, there is room for improvement in the reduction of the ferrite count within the weld region. The amount of ferrite within the weld is highly dependent, not only on the material composition but also the cooling rate. Fast cooling rates retain more of the ferrite that forms at elevated temperature [38]. Reducing the risk of producing very high ferrite levels in the weld requires a reduced heat input and therefore a maximum cooling rate. Therefore, future work will focus on adjusting the WPS to reduce the heat input and to improve the penetration during AM [39].

ACKNOWLEDGMENT

We are very grateful to Ben Crutchley from Industrial 3D Robotics, Fotios Papadopoulos from Shadow Robotics company, Ben Kitchener, Kieren Howarth and Samuel Edwards from the Enabling Sciences for Intelligent Manufacturing group from the Physics and Astronomy department and Jon Willmott and Nicholas Boone from the Electronic and Electrical Engineering department at the University of Sheffield for their help and their invaluable support. The team gratefully acknowledge Innovate-UK for the funding of the SERFOW project (project number 103462).

REFERENCES

[1] W. E. Frazier, "Metal additive manufacturing: a review," *Journal of Materials Engineering and Performance*, vol. 23, no. 6, pp. 1917–1928, 2014.

[2] A. Standard, "F2792-12a, 2012,," *Standard terminology for additive manufacturing technologies*, vol. 10.

[3] I. Gibson, D. W. Rosen, B. Stucker, *et al.*, *Additive manufacturing technologies*. Springer, 2014, vol. 17.

[4] S. W. Williams, F. Martina, A. C. Addison, J. Ding, G. Pardal, and P. Colegrove, "Wire+ arc additive manufacturing," *Materials Science and Technology*, vol. 32, no. 7, pp. 641–647, 2016.

[5] Z. Pan, J. Polden, N. Larkin, S. Van Duin, and J. Norrish, "Recent progress on programming methods for industrial robots," in *ISR 2010 (41st International Symposium on Robotics) and ROBOTIK 2010 (6th German Conference on Robotics)*. VDE, 2010, pp. 1–8.

[6] M. Baumers, R. Wildman, M. Wallace, J. Yoo, B. Blackwell, P. Farr, and C. J. Roberts, "Using total specific cost indices to compare the cost performance of additive manufacturing for the medical devices domain," *Proceedings of the Institution of Mechanical Engineers, Part B: Journal of Engineering Manufacture*, vol. 233, no. 4, pp. 1235–1249, 2019.

[7] J. Allen, "An investigation into the comparative costs of additive manufacture vs. machine from solid for aero engine parts," ROLLS-ROYCE PLC DERBY (UNITED KINGDOM), Tech. Rep., 2006.

[8] K. Schreve, H. Schuster, and A. Basson, "Manufacturing cost estimation during design of fabricated parts," *Proceedings of the Institution of Mechanical Engineers, Part B: Journal of Engineering Manufacture*, vol. 213, no. 7, pp. 731–735, 1999.

[9] R. French, H. Marin-Reyes, and M. Benakis, "Transfer analysis of human engineering skills for adaptive robotic additive manufacturing in the aerospace repair and overhaul industry," in *International Conference on Applied Human Factors and Ergonomics*. Springer, 2018, pp. 3–12.

[10] Shadow robotics company ltd, introducing the new modular grasper. [Online]. Available: https://www.shadowrobot.com/products/modular-grasper/

[11] N. Pestell, L. Cramphorn, F. Papadopoulos, and N. Lepora, "A sense of touch for the shadow modular grasper," *IEEE Robotics and Automation Letters*, 2019.

[12] Industrial 3D Robotics, Phobos, url = http://i3drobotics.com/phobos, note= Accessed: 04 January 2019.

[13] E. Mouaddib, J. Batlle, and J. Salvi, "Recent progress in structured light in order to solve the correspondence problem in stereovision," in *Robotics and Automation, 1997. Proceedings., 1997 IEEE International Conference on*, vol. 1. IEEE, 1997, pp. 130–136.

[14] B. Tippetts, D. J. Lee, K. Lillywhite, and J. Archibald, "Review of stereo vision algorithms and their suitability for resource-limited systems," *Journal of Real-Time Image Processing*, vol. 11, no. 1, pp. 5–25, 2016.

[15] X. Corts and F. Serratosa, "An interactive method for the image alignment problem based on partially supervised correspondence," *Expert Systems with Applications*, vol. 42, no. 1, pp. 179 – 192, 2015. [Online]. Available: http://www.sciencedirect.com/science/article/pii/S0957417414004588

[16] R. Bogue, "Robots in the nuclear industry: a review of technologies and applications," *Industrial Robot: An International Journal*, vol. 38, no. 2, pp. 113–118, 2011.

[17] S. Kawatsuma, M. Fukushima, and T. Okada, "Emergency response by robots to fukushima-daiichi accident: summary and lessons learned," *Industrial Robot: An International Journal*, vol. 39, no. 5, pp. 428–435, 2012.

[18] M. Quigley, K. Conley, B. Gerkey, J. Faust, T. Foote, J. Leibs, R. Wheeler, and A. Y. Ng, "Ros: an open-source robot operating system," in *ICRA workshop on open source software*, vol. 3, no. 3.2. Kobe, Japan, 2009, p. 5.

[19] L. Li, Z. Wang, F. Pei, and X. Wang, "Improved illumination for vision-based defect inspection of highly reflective metal surface," *Chinese Optics Letters*, vol. 11, 02 2013.

[20] Z. Zhang, H. Yoshioka, T. Imamura, and T. Miyake, "Optimization of light-source position in appearance inspection for surface with specular reflection," in *2013 IEEE International Conference on Information and Automation (ICIA)*. IEEE, 2013, pp. 602–607.

[21] H. Golnabi and A. Asadpour, "Design and application of industrial machine vision systems," *Robotics and Computer-Integrated Manufacturing*, vol. 23, no. 6, pp. 630–637, 2007.

[22] TWI. Vision system for monitoring and control of arc welding. [Online]. Available: https://www.twiglobal.com/technicalknowledge/job-knowledge/visionsystemformonitoringandcontrolofarcwelding138

[23] R. French and H. Marin-Reyes, "Underpinning uk high-value manufacturing: development of a robotic re-manufacturing system," in *Emerging Technologies and Factory Automation (ETFA), 2016 IEEE 21st International Conference on*. IEEE, 2016, pp. 1–8.

[24] A. Billard, S. Calinon, R. Dillmann, and S. Schaal, *Robot Programming by Demonstration*. Berlin, Heidelberg: Springer Berlin Heidelberg, 2008, pp. 1371–1394. [Online]. Available: https://doi.org/10.1007/978-3-540-303015_60

[25] R. French, A. Cryer, G. Kapellmann-Zafra, and H. Marin-Reyes, "Evaluating the radiation tolerance of a robotic finger," in *Annual Conference Towards Autonomous Robotic Systems*. Springer, 2018, pp. 103–111.

[26] R. French, H. MarinReyes, and E. Kourlitis, "Usability study to qualify a dexterous robotic manipulator for high radiation environments," in *Emerging Technologies and Factory Automation (ETFA), 2016 IEEE 21st International Conference on*. IEEE, 2016, pp. 1-6.

[27] ROS for LabVIEW by Tufts University, url = www.clearpathrobotics.com/assets/guides/ros/ROSforLabVIEW.html, Accessed: 04 January 2019.

[28] A. Narayanamoorthy, R. Li, and Z. Huang, "Creating ros launch files using a visual programming interface," in *2015 IEEE 7th International Conference on Cybernetics and Intelligent Systems (CIS) and IEEE Conference on Robotics, Automation and Mechatronics (RAM)*. IEEE, 2015, pp. 142–146.

[29] S. Edwards and C. Lewis, "Ros-industrial: applying the robot operating system (ros) to industrial applications," in *IEEE Int. Conference on Robotics and Automation, ECHORD Workshop*, 2012.

[30] Dynasty 350 owner's manual. [Online]. Available: https://www.millerwelds.com/files/ownersmanuals/o216869ah_mil.pdf

[31] ISO-6520-1:2007, "Welding and allied processes Classification of geometric imperfections in metallic materials Part 1: Fusion welding," International Organization for Standardization, Tech. Rep., 2007. [Online]. Available: https://www.iso.org/standard/62521.html

[32] ISO-5817, "Welding Fusion-welded joints in steel, nickel, titanium and their alloys (beam welding excluded) Quality levels for imperfections," International Organization for Standardization, Tech. Rep., 2014. [Online]. Available: https://www.iso.org/standard/54952.html

[33] T. Kuroda, K. Ikeuchi, and Y. Kitagawa, "Role of austenite in weld toughness of super duplex stainless steel," *Welding in the World*, vol. 49, no. 5-6, pp. 29–33, 2005.

[34] C. G. Camerini, V. M. A. Silva, I. A. Soares, R. W. F. Santos, J. E. Ramos, J. M. C. Santos, and G. R. Pereira, "Ferrite content meter analysis for delta ferrite evaluation in superduplex stainless steel," *Journal of Materials Research and Technology*, vol. 7, no. 3, pp. 366–370, 2018.

[35] J. A. Willmott, *Dynamics of regenerative heat transfer*. CRC Press, 2001.

[36] EN288-3:92AMD197, "Specification and approval of welding procedures for metallic materials-welding procedure test for the arc welding of steels," NF EN, Tech. Rep., 2013. [Online]. Available: https://standards.globalspec.com/std/767677/EN%20288-3

[37] ASTM-A789/A789M18, "Standard Specification for Seamless and Welded Ferritic/Austenitic Stainless Steel Tubing for General Service," ASTM International, Tech. Rep., 2018. [Online]. Available: https://www.astm.org/Standards/A789.htm

[38] TWI. Duplex stainless steel. part 1 duplex stainless steel part 1. [Online]. Available: https://www.twiglobal.com/technical-knowledge/job-knowledge/duplex-stainless-steel-part-1-105

[39] Sandvik. Improved corrosion performance in super-duplex welds. [Online]. Available: https://www.materials.sandvik/en/knowledge-center/oil-and-gas/improved-corrosion-performance-in-super-duplex-welds/